Supporting Information

Structure and Crystallization Behavior of Aqueous KCl-$MgCl_2$ Solutions

Yifa Du[a,b], Yanan Wu[b], Xu Zhao[b], Jianrong Zeng[c], Yunxia Wang[b], Lingzong Meng[a,*], Hongyan Liu[b], Yongquan Zhou[b], Fayan Zhu[b,*]

[a] School of Chemistry and Chemical Engineering, Linyi University, Linyi 276000, China.

[b] Key Laboratory of Comprehensive and Highly Efficient Utilization of Salt Lake Resources; Key Laboratory of Salt Lake Resources Chemistry of Qinghai Province; Qinghai Institute of Salt Lakes, Chinese Academy of Sciences, Xining, Qinghai 810008, China.

[c] Shanghai Synchrotron Radiation Facility, Shanghai Advanced Research Institute, Chinese Academy of Sciences, 201204 Shanghai, P. R. China.

Part 1. X-ray data calibration process

The F scattering vector Q = 4π sinθ / λ has a maximum value of 21 $Å^{-1}$. After corrections for polarization, the Bremsstrahlung radiation component of the X-ray beam, absorption by the sample, multiple scattering, fluorescence, and Compton scattering, as well as air background and empty capillary scattering, the simplified data were scaled to the self-scattering oscillations of the sample and normalized to the single-atom scattering F(Q).

$$F(Q) = \sum_{\alpha} \sum_{\beta \geq \alpha} (2 - \delta_{\alpha\beta})\, c_{\alpha} c_{\beta} f_{\alpha}(Q) f_{\beta}(Q) [S_{\alpha\beta}(Q) - 1] \qquad (1)$$

The scattering vector Q = 4πsinθ/λ, λ is the X-ray wavelength, θ is the half-scattering angle; c_{α} and c_{β} are the concentrations of α and β atoms; $f_{\alpha}(Q)$ and $f_{\beta}(Q)$ are the X-ray scattering form factors of the atoms; ρ is the density of the solution; δαβ is the Kronecker function; and $S_{\alpha\beta}(Q)$ is the bias structural factor, which is given in the following expression:

$$S_{\alpha\beta}(Q) - 1 = 4\pi\rho \int_{0}^{\infty} r^2 (g_{\alpha\beta}(r) - 1) \frac{sinQr}{Qr}\, dr \qquad (2)$$

$$g_{\alpha\beta}(r) = \frac{n_{\alpha\beta(r)}}{c_{\beta}\rho 4\pi r 2dr} \qquad (3)$$

Where $n_{\alpha\beta}(r)$ is the coordination number of the β-atom centered on the α-atom in the range r to r+dr in the skew-radial distribution function.

The experimentally obtained F(Q) is Fourier transformed to obtain the structure-function G(r):

$$G(r) = \frac{1}{(2\pi)3\rho} \int_{Qmin}^{Qmax} 4\pi Q 2F(Q) \frac{sinQr}{Qr} dQ \qquad (4)$$

Part 2. Details of EPSR modelling

Table S1. EPSR simulation boxes setup details

	KC25-MC0	KC11-MC14	KC6-MC21	KC0-MC35
Number of K^+ ions	79	34	19	-
Number of Mg^{2+} ions	-	36	54	102
Number of Cl^- ions	79	106	127	204
Number of water molecules	1000	1000	1000	1000
Length of box (Å)	30.6	31.7	31.7	32.1
Atomic number density (atom $Å^{-3}$)	0.0926	0.0958	0.0964	0.0951

Table S2. Reference potential parameters used in EPSR modelling[1-3]

	Charge	Mass	ε (kJ • mol^{-1})	σ (Å)
K	1.0000	39.0980	0.5216	3.2500
Mg	2.0000	24.3050	0.7750	1.5980
Cl	-1.0000	35.4530	0.5660	4.1910
OW	-0.8476	15.9999	0.6500	3.1600
OH	0.4238	2.0000	0	0

Part 3. Raman spectroscopy experiment

This experiment used Thermo Company's DXR Raman spectrometer, and the excitation wave-length of the semiconductor laser was 532 nm. The laser beam through the microscope objective lens was focused on a sample. The laser spot diameter was about 1.1 μm, and the 10 x objective lens was used for spectra measurements. The scattered light generated by sample excitation passed through a 4000 g/mm grating, then through a 532 nm filter to remove Ray-leigh scattered rays, and was finally detected by a charge-coupled device detector. The spectral resolution was about 1 cm^{-1}, and the wavenumber accuracy was ±0.3 cm^{-1}. The output power of the laser was 8 mW, the spectral scanning range was set to 400-4000 cm^{-1},30 cumulative scans were used, and the exposure time was 10 s. Before the experiment, the beam collimation, and spectral frequency of the spectrometer was calibrated.

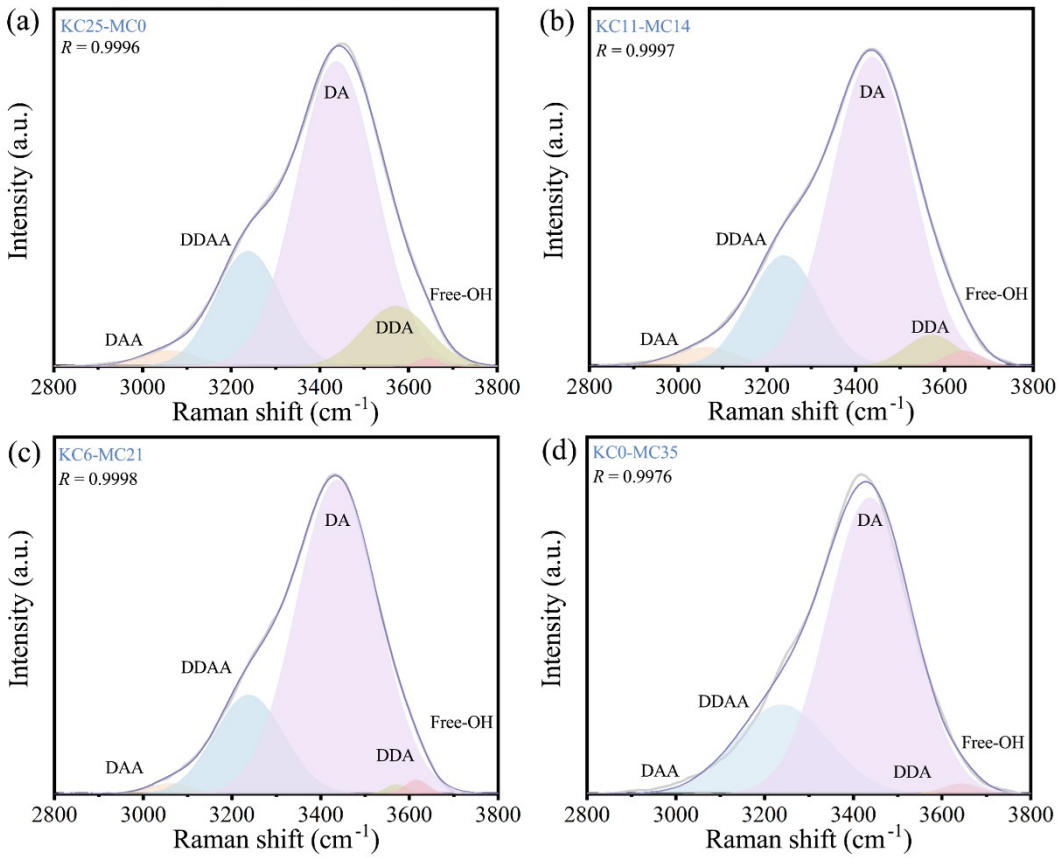

Fig.S1 Schematic diagram of Raman peak results of KCl-$MgCl_2$ mixed solutions with different mass fractions

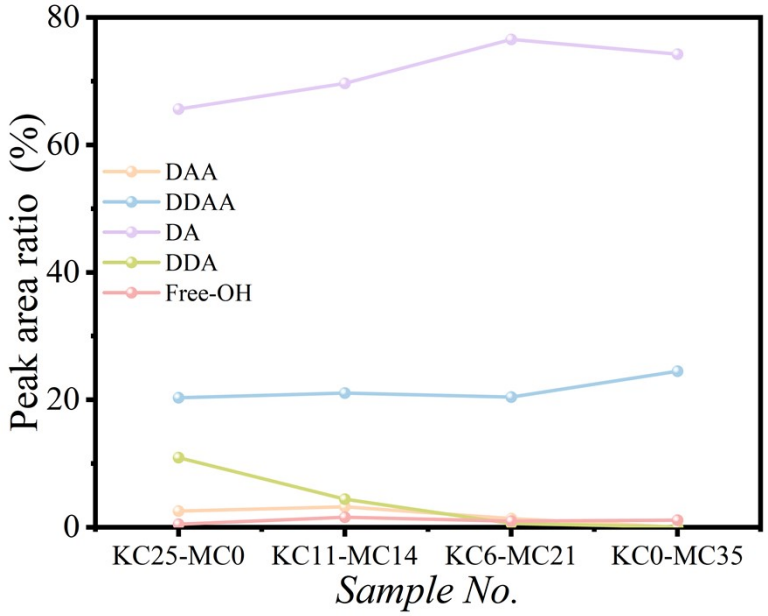

Fig.S2 Changes in OH stretching vibration structure of KCl-$MgCl_2$ mixed solutions with different mass fractions

Part 4. Molecular Dynamics Simulation

To confirm the accuracy of the MD simulation, This work used different force fields to test the density of different samples, as shown in Table S3.

Table S3. MD simulation and actual density of different samples under different force fields

Force field	Density (KC25-MC0)	Density (KC11-MC14)	Density (KC0-MC35)
Opls-AA	1136.43 kg/m^3	1173.77 kg/m^3	1285.87 kg/m^3
Amber99sb-ildn.ff	1138.76 kg/m^3	1163.1 kg/m^3	1277.23 kg/m^3
AmberGS.ff	1130.46 kg/m^3	1158.28 kg/m^3	1278.48 kg/m^3
Charmm27.ff	1191.69 kg/m^3	1211.25 kg/m^3	1364.33 kg/m^3
Actual measurement at 25 ℃	1163.1 kg/m^3	1198.47 kg/m^3	1325 kg/m^3

Table S4. Details of the simulation box at different concentration of KCl-$MgCl_2$ solutions.

Sample	n_K	n_{Mg}	n_{Cl}	n_{water}	V(nm^3)
KC25-MC0	2000	0	2000	25400	10×10×10
KC11-MC14	840	900	2640	25020	10×10×10
KC6-MC21	474	1320	3114	24420	10×10×10
KC0-MC35	0	2294	4588	22382	10×10×10

Table S5. Partial electric charge sets and Lennard-Jones parameters for the OPLS-AA force field.

	Charge	Mass	ε (kJ·mol^{-1})	σ (Å)
K	1.0000	39.0983	0.001372	0.4935
Mg	2.0000	24.3050	3.6612	0.1645
Cl	-1.0000	35.4530	1.2552	0.3400
OW	-0.820	15.9994	0.6500	3.1600
OH	0.4100	1.0080	0	0

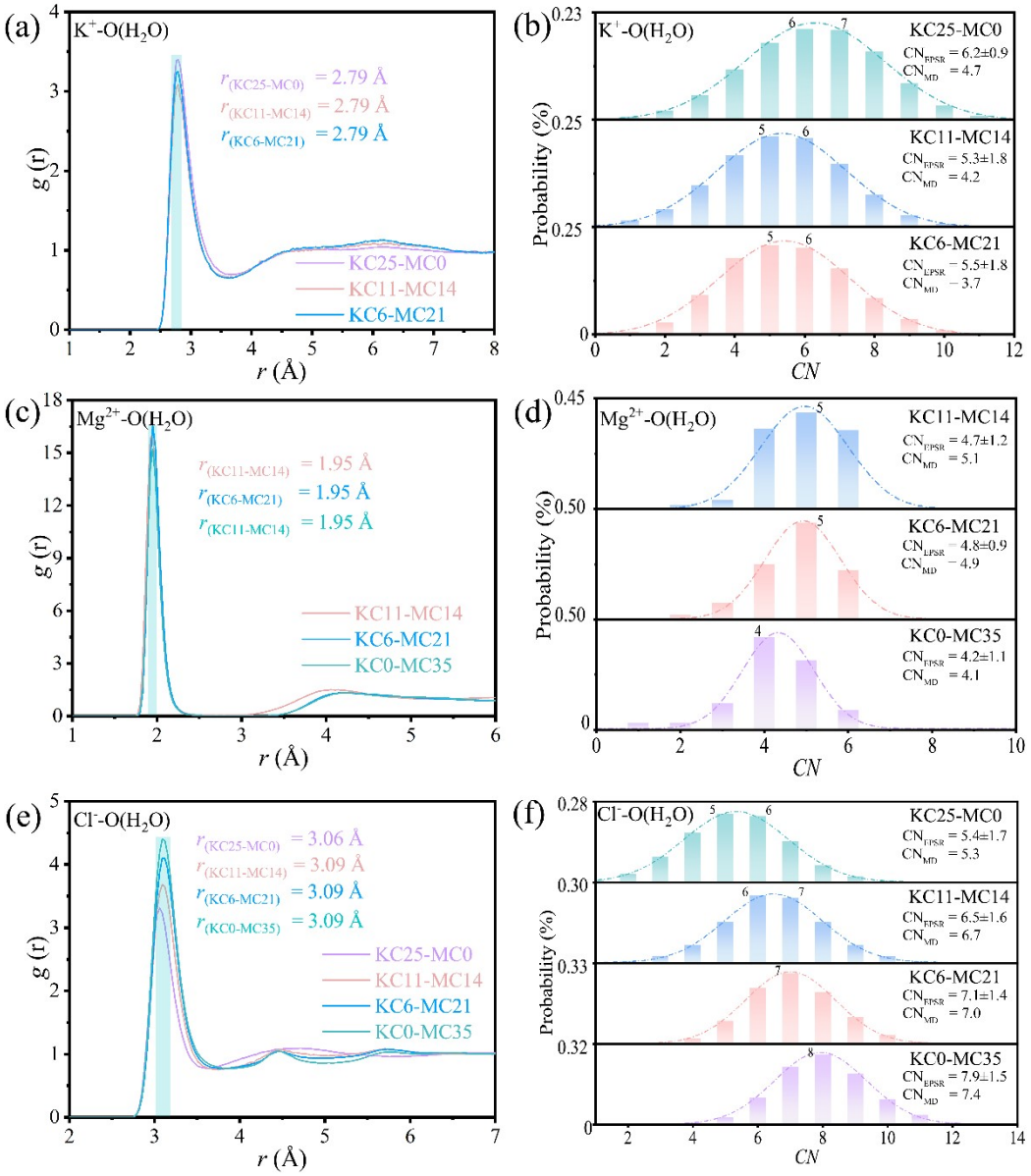

Fig.S3 Pair distribution functions and coordination numbers of K^+-O(H_2O), Mg^{2+}- O(H_2O), and Cl^- - O(H_2O) atomic pairs in KCl-$MgCl_2$ solution, simulated by EPSR (solid line) and MD (dashed line)

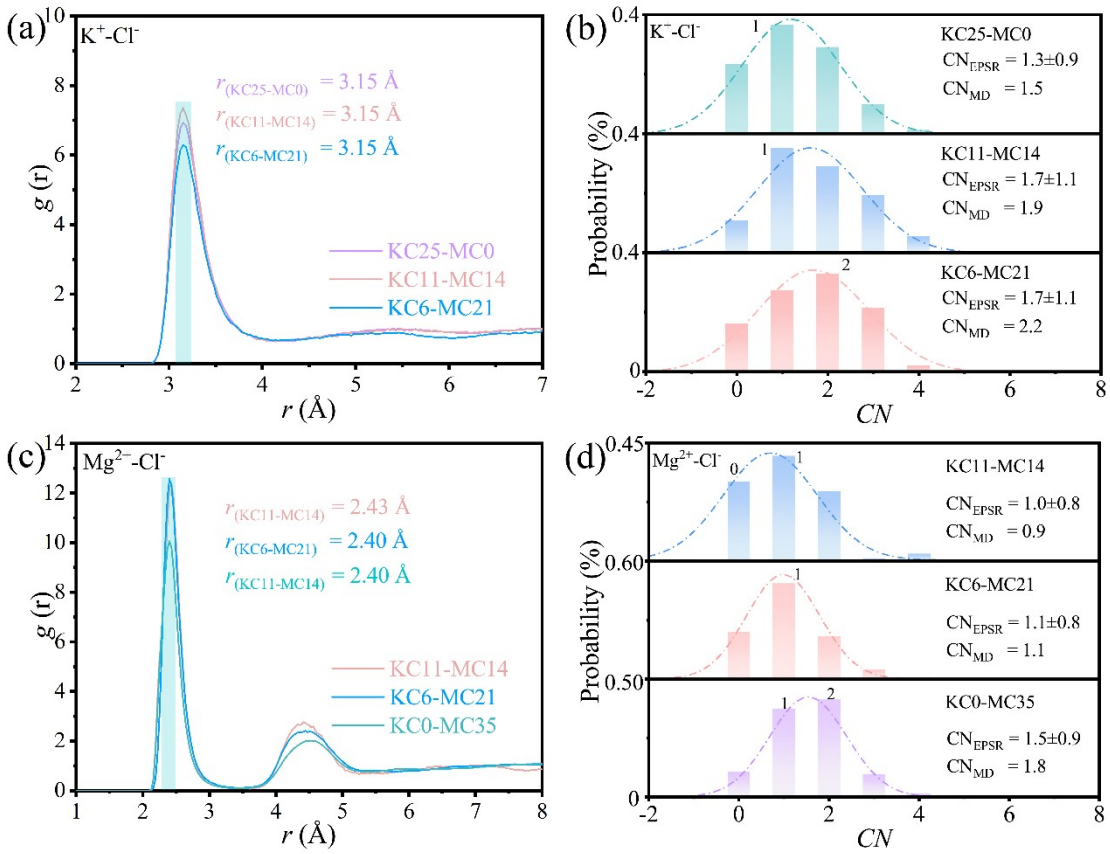

Fig.S4 Pair distribution function and coordination number of K^+- Cl^- and Mg^{2+}- Cl^- in mixed solution, EPSR simulation (solid line), MD simulation (dashed line)

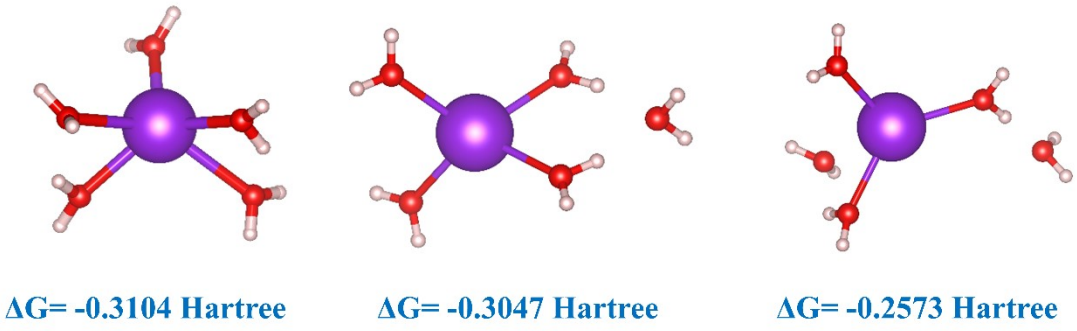

Fig.S5 Hydration energy of different potassium ion clusters. Color: Red O, Pink H, Purple K.

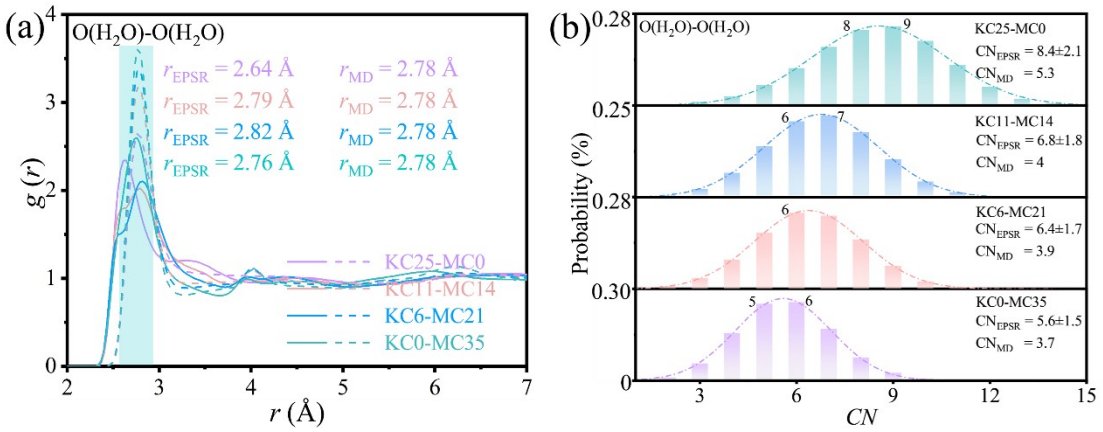

Fig.S6 Pair distribution function and coordination number of O (H_2O) - O (H_2O) in mixed solution, EPSR simulation (solid line), MD simulation (dashed line)

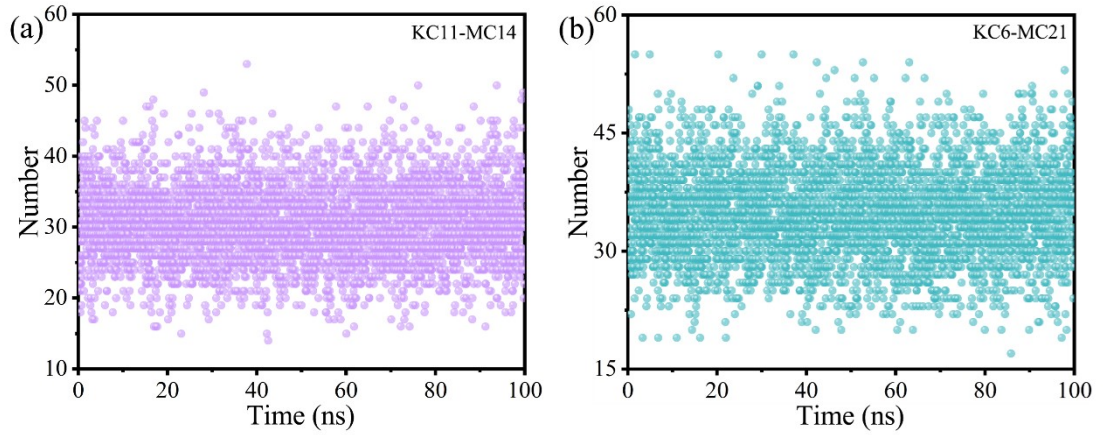

Fig.S7 The number of three-ion clusters at different times

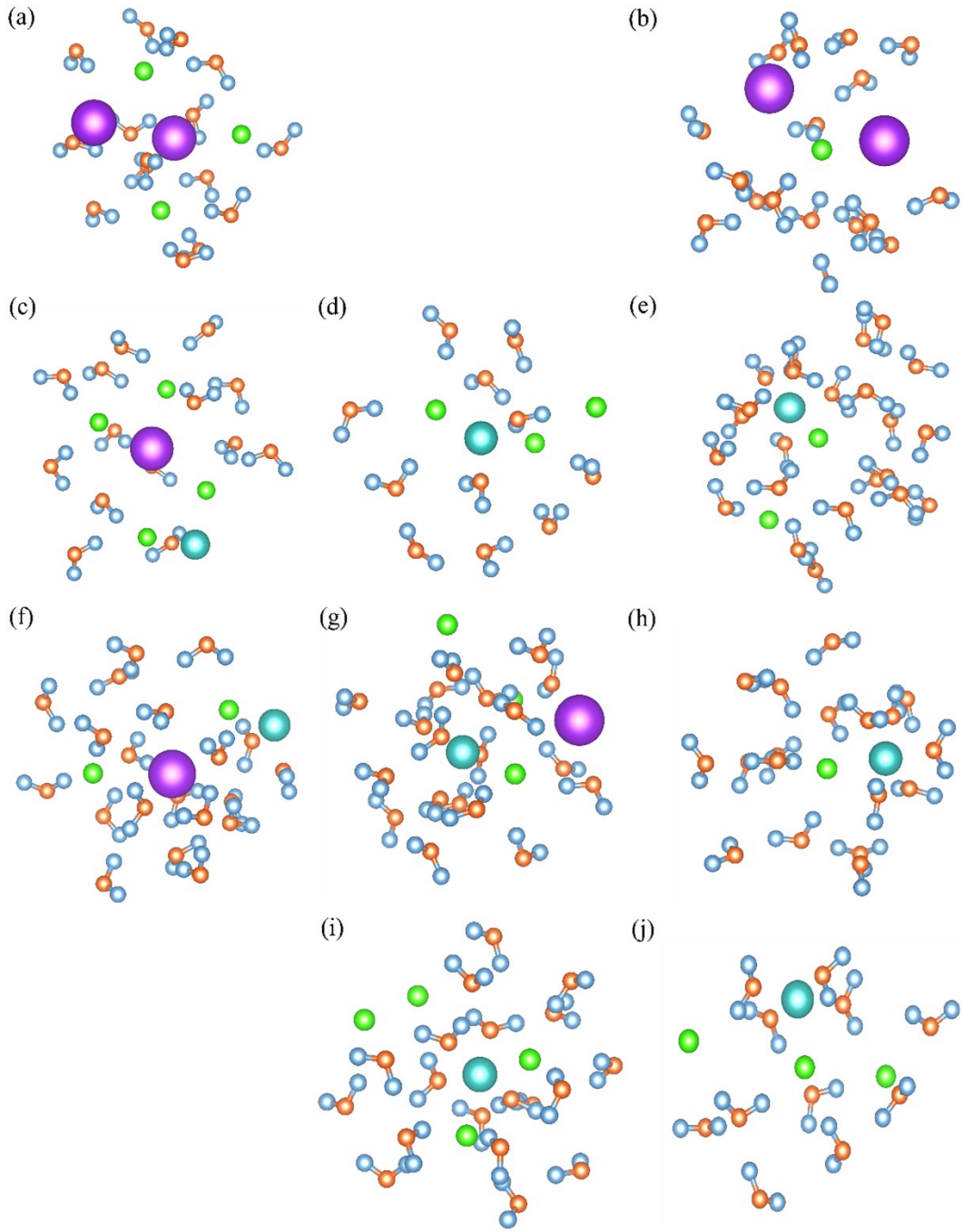

Fig.S8 MD simulation snapshots of solutions with different mass fractions (a) - (b) KC25-MC0, (c) - (e) KC11-MC14, (f) - (h) KC6-MC21, (i) - (j) KC0-MC35 at 75ns, centered around K^+, Mg^{2+}, and Cl^- within a range of 5 Å. Color: Orange O, Blue H, Green Cl, Blue Mg, Purple K.

Part 5. Infrared Spectroscopy Experiment

The gas regulation system comprises two nitrogen branches: dry and wet nitrogen, which are introduced through a humidifier. These gases subsequently traverse two distinct gas mass flow meters, ensuring precise control over the flow rates of both dry and wet nitrogen. This meticulous control facilitates the modulation of the relative humidity (RH) within the sample pool.

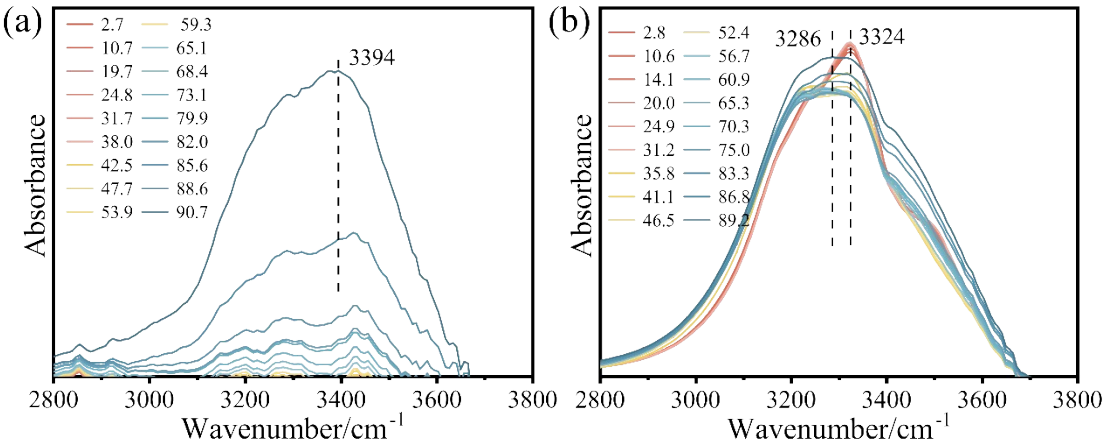

Fig.S9 Infrared spectra of KCl solution droplets (a) and KCl-$MgCl_2$ mixed solution droplets (b) during the process of humidity rise

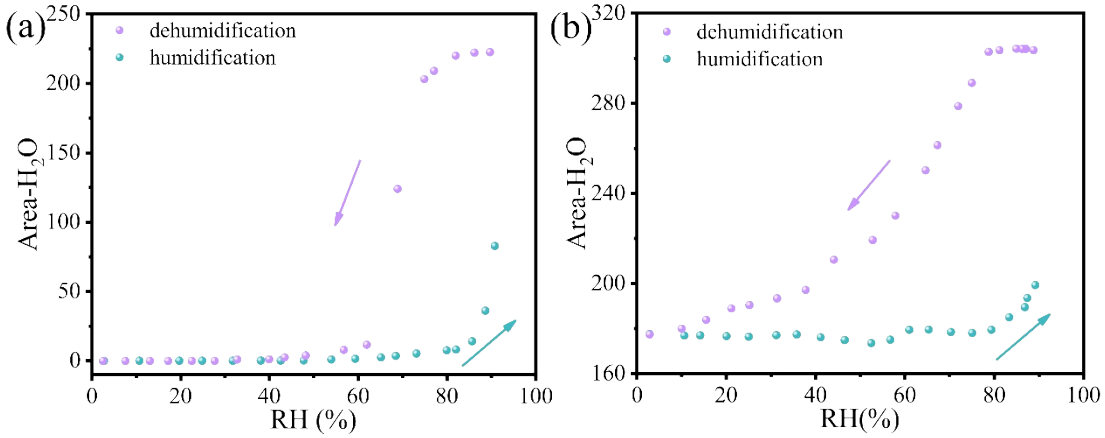

Fig.S10. Water peak areas of KCl solution droplets (a) and KCl-$MgCl_2$ mixed solution droplets (b) during humidity decrease and increase

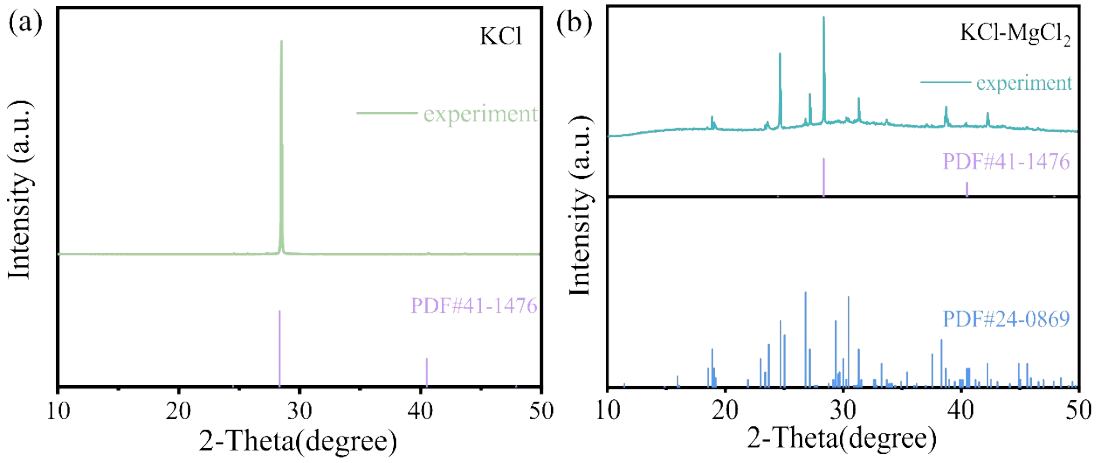

Fig.S11 X-ray diffraction pattern of crystalline product

Part 6. Study on Crystallization Behavior of Solution

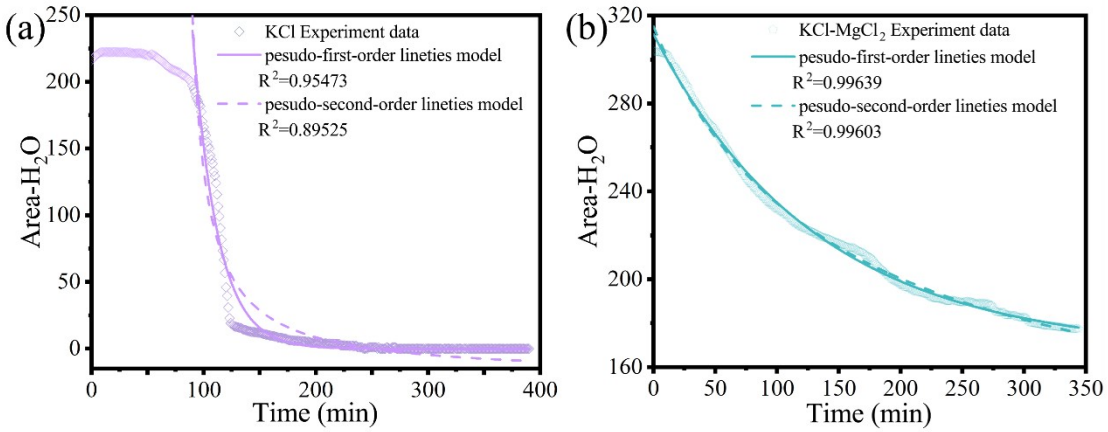

Fig.S12 Water peak area variation curves of KCl droplets (a) and KCl-$MgCl_2$ mixed solution droplets (b) at different times

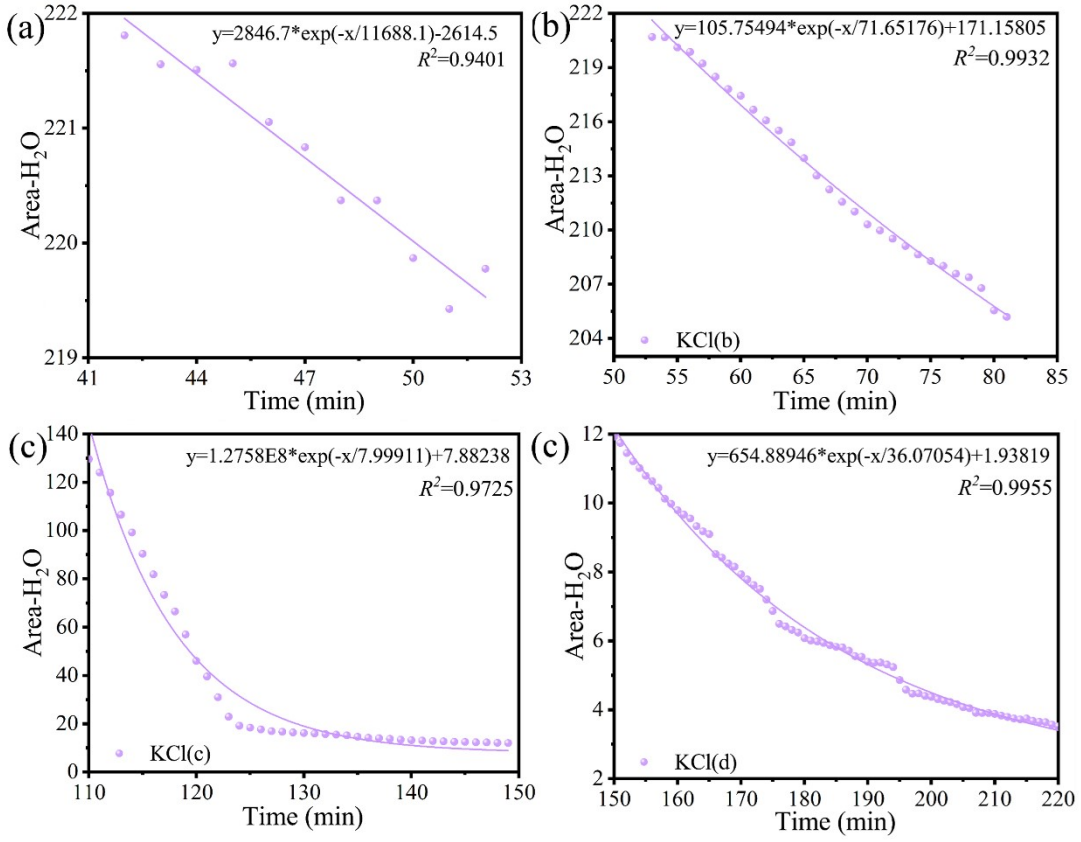

Fig.S13 Fitting curves of water peak area changes at different stages of KCl solution droplets at different times

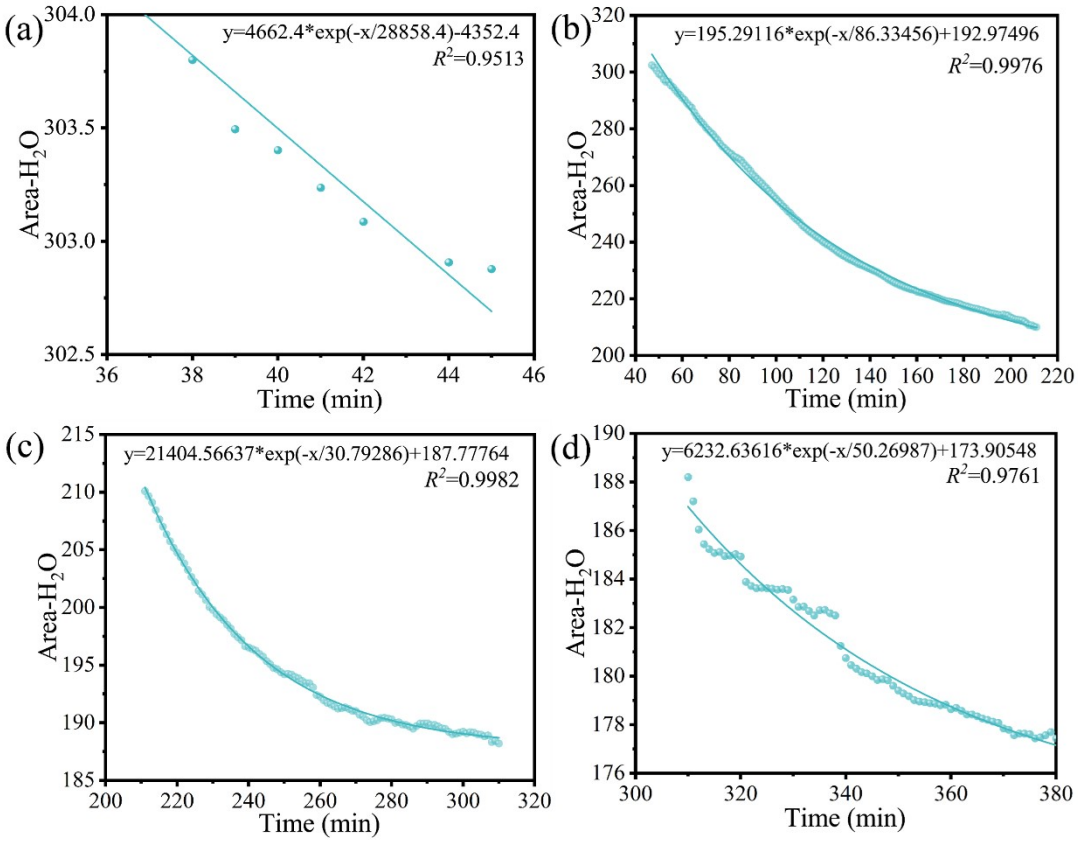

Fig.S14 Fitting curves of water peak area changes at different stages of KCl-$MgCl_2$ mixed solution droplets at different times

Table S6 Reaction kinetics equations and corresponding parameters at different stages

Solution droplets	Stage	Equation	Correlation coefficient	Rate constant (s^{-1})
KCl	a	y=2846.657*exp(-x/11688.06389)-2614.49202	0.9410	~0
	b	y=105.75494*exp(-x/71.65176)+171.15805	0.9932	0.0140
	c	y=1.2758E8*exp(-x/7.99911)+7.88238	0.9725	0.1250
	d	y=654.88946*exp(-x/36.07054)+1.93819	0.9955	0.0277
KCl-$MgCl_2$	a	y=4662.367*exp(-x/28858.4397)-4352.41088	0.9513	~0
	b	y=195.29116*exp(-x/86.33456)+192.97496	0.9976	0.0116
	c	y=21404.56637*exp(-x/30.79286)+187.77764	0.9982	0.0325
	d	y=6232.63616*exp(-x/50.26987)+173.90548	0.9761	0.0199

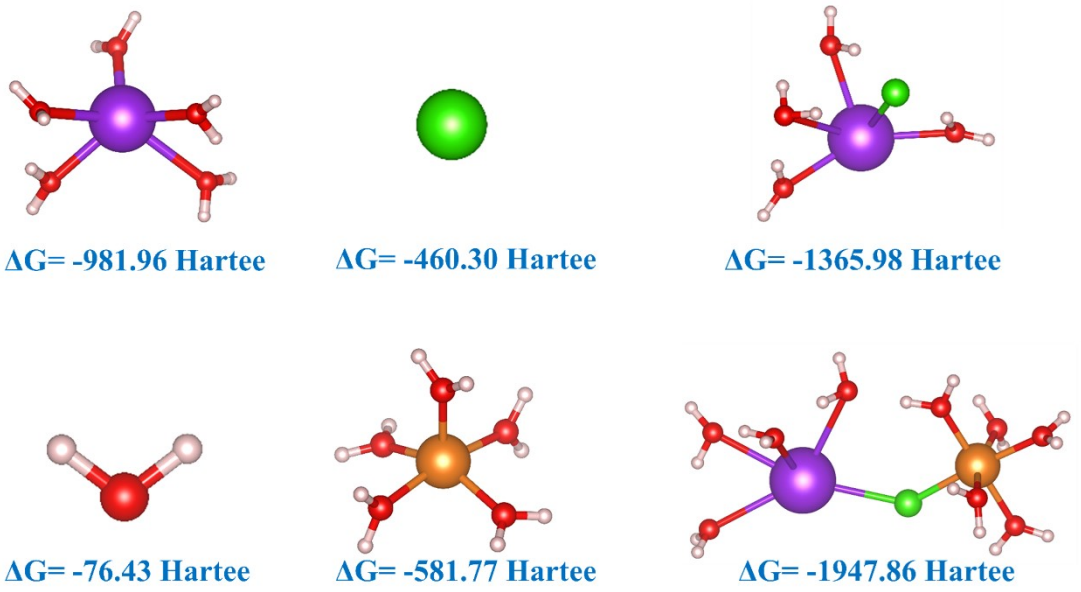

Figure S15. Gibbs free energies of different clusters calculated by DFT. Color: Red O, Pink H, Green Cl, Orange Mg, Purple K.

References

1. Y. Wang, G. Wang, D. T. Bowron, F. Zhu, A. C. Hannon, Y. Zhou, X. Liu and G. Shi, *Phys. Chem. Chem. Phys*, 2022, **24**, 22939-22949.
2. H. Liu, Y. Zhou, D. An, G. Wang, F. Zhu and T. Yamaguchi, *J. Phys. Chem. B*, 2022, **126**, 5866-5875.
3. Z. Jing, Y. Zhou, T. Yamaguchi, K. Yoshida, K. Ikeda, K. Ohara and G. Wang, *J. Phys. Chem. Lett*, 2023, **14**, 6270-6277.